Stability and Convergence Analysis of Casson-nano Fluid Flow is Heated Non-linearly with Viscous Dissipation with Convective Boundary Conditions

G.Mahanta[1], S.Mohanta[2], D. Mohanty[3]

[1,2,3]*Department of Mathematics C. V. Raman Global University, Bhubaneswar-752054, India.*

Abstract

This work uses a non-linear stretching surface with viscous dissipation in two dimensions to show the influence of heat absorption and suction on magneto-hydrodynamic boundary-layer flow of Casson nanofluid. The leading PDEs are turned into a set of ODEs with sufficient boundary conditions using similarity transformations, and then numerically resolved using a BVP4C software technique. The model is enforced for nano-fluid which extension the feeling of thermophoresis and Brownian motion. The influence of dimensionless control settings on nanoparticle concentration profiles, temperature, and flow velocity is investigated using graphs. Other important properties, such as the skin friction coefficient, heat, and mass transport in a variety of conditions, and the relationship between these factors, are examined using tables and graphs.Stability and convergence analysis model has been utilized.The initial value of different parameters are given below as

$$U = V = T = C = 0, \Delta\eta = 0.007, \Delta x = 0.9, \Delta y = 0.39,$$
$$E_c \geq 0.225, P_r \geq 0.467, N_t \geq 0.556$$

Furthermore, the numerical computations and previously published research are proven to be in perfect agreement.

Keywords: Casson nanofluid, Magnetic field,heat absorption,

INTRODUCTION

Because of its enormous illustration of uses, the investigation of non-Newtonian liquids over an expanding surface has accomplished incredible consideration. Truth be told, the effects of non-Newtonian conduct can be surveyed by its versatility, yet their constitutive conditions here and there recognize the rheological properties of the liquid.Given the rheological boundaries, the constitutive conditions in the non-Newtonian liquids are more perplexing and accordingly bringing about the convoluted conditions than the Navier–Stirs up conditions.A significant number of the fluids have been used in the oil area, multiplex organizations, cooling cycles of miniature boats, open-stream exchanging, and reproducing repositories are impressive [1–5]. The fluid performs both shear-subordinate consistency as well as shear-subordinate thickness in various forms. The deliberate effects of several quantities on the progression of Casson fluid was

investigated [6]. The liquid has unique attributes in the class of non-Newtonian liquids which are ordinarily utilized in fabricating, boring, several designing exercises in biological fields [7] . Mukhopadhyay et al. [8] presented effects of the gaseous exchange within the sight of a substance response on the stream of the several liquids. Pramanik [9] investigated the effect of thermal radiation over exponentially stretching sheet. Mahanta et al. [10] investigated the boundary layer flow of the fluid having electrical field over exponentially stretching sheet. Khalid et al. [11] investigated the numerical solution of different solution of nano fluid and compared the isothermal solution graphically.While, casson fluid of several convection streaming over a vertical surface in a permeable medium was anlysed [12]. Nadeem et al. [13] investigated the MHD three dimensional using convective boundary condition to find out the casson nano fluid. Shaw et al.[14] illustrated the effect of heat and mass transfer on the unsteady MHD casson fluid which chemically reactive in a porous platform upon a stretching sheet. Zhu et al. [15] analyzed heat transfer with the help of radiation and MHD flow. Sanjaya and khan [16] carried out the boundary layer fluid flow and effect of various parameters in the effect of thermal radiation and magnetic field on the flow of casson fluid stretching surface. Choi [17] was the first scientist who had reported the enhancement of thermal capabilities of nanofluids. Khalid et al. [18] investigated the impact of the hotness supply on consistent stream and hotness communicate over a dramatically growing chamber over its spiral way. Anwar et al.[19] studied simultaneous impact of not only heat and but also mass transfer of various types of nano fluids in a non-liner stretching sheet. Imtiaz et al. [20] examined several transformation for numerical solutions. Oyelakin et al. [21] checked out the blended stream that made by an extending chamber . Afify [22] examined several mathematical solutions for nanofluid as well as the effects of several parameters on the casson nanofluid . Ibrahim et al. [23] mathematically inspected the impacts of a compound receptive stream and a gooey scattering on CNF and hotness transmission across an growing region. Shah et al. [24] investigated different fluids that are used in human body that blended convective streaming in with the synthetically responsive conjugate sources. Several neoteric explores connected with an investigation of [25–28].

Different investigations are connected with the assessment of the impacts of smooth movements over the assorted surfaces

in Newtonian and non-Newtonian sorts. Now a days, various investigations have been performed to investigate various sorts of stream and warm effects of nanofluid stream over different types of surfaces. Ferdows et al.[29] investigated the numerical method of boundary layer flow of different types of nano fluid with viscous dissipation. Khan and pop [30] investigated the numeric solution of the nano fluid that stretching over a flat surface. MHD or hydrodynamic has different properties leading truth. The collaboration among liquids and fero attractive particles electromagnetic field. Accordingly the electromagnetic elements, Maxwell condition were consolidated through the liquid condition [31-33]. The irreversible interaction through which the work done by a liquid on adjoining layers because of the activity of powers was changed into heat which was characterized as scattering. The coherence and nuclear power balance on a differential component fixed in an unadulterated streaming liquid the Reedy artle on the impact of dispersal and MHD over the stream [34]. Salem article on the impact of variable consistency dissemination and substance response on hotness and mass change stream of MHD.thermopedesis is the caused movement of fluids of atoms. This is became overhaul temperature slope. The operant Of consistent temperature angle liquid progression of the slope movement. As of late numerous analyst included Thermo parsing and Brownian movement [35-39]. Mohanta article found the irreversible examination of 3D case with nonlinear warm radiation.

Convective limit condition generally utilized because of numerous significant application, for example, strong networks miniature change of cooling, molecule chomps and so forth convective limit condition is the consistently connected with the hotness. Eid et al. [41] assessed several effects of sources (sink) that are not stable in the formation of a nanofluid in a permeable state. Eid et al. [42] tended to the consistent several fluid stream and hotness transport past a non-straightly growing plate with the hotness age (ingestion) in a permeable state and that checked the effect of the attractive boundary on the two-stage nanofluid through a penetrable extending plate. More related works according to these components [43–45].

PROBLEM STRUCTURE

Consider MHD CNF flow in the area $y > 0$ as a $2D$ viscous flow over an exponentially extensible surface. Under the influence of viscous dissipation, thermal expansion and heat source,the fluid remains stable compressible.The extensible sheet is designed to have a power law global velocity profile. $u_w(x) = ax^n$ where a and n are positive constant. The magnetic field's activity is subjected to variable strength $B(x) = B_0 x^{\frac{n-1}{2}}$. Although there is no electric field, the resulting magnetic field was ignored by Reynold's weak magnetic number. $T_w(x) = T_\infty + Ax^n$ and $C_w(x) = C_\infty + Ax^n$ denotes the temperature and concentration of the surface where $A > 0$ is the fixed value,

T_∞ denotes free stream temperature and C_∞ is the ambient nano particle concentration.
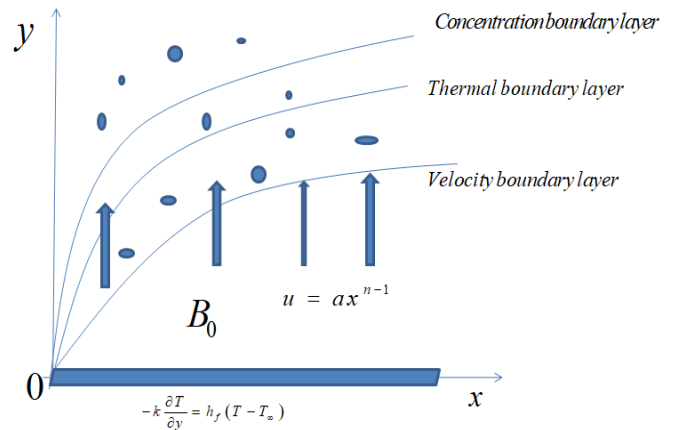

Fig. 1. Schematic representation

MATHEMATICAL FORMULATION

Consider MHD CNF stream over a dramatically extendable, hence the governing equations obtained as follows;

$$\frac{\partial u}{\partial x} + \frac{\partial u}{\partial y} = 0 \tag{1}$$

$$u\frac{\partial u}{\partial x} + v\frac{\partial u}{\partial y} = v(1 + \frac{1}{\beta}) - \frac{\partial^2 u}{\partial y^2} - \frac{\sigma B^2(x)}{\rho_f}u \tag{2}$$
$$+ g\beta_c(c - c_\infty) + g\beta_T(T - T_\infty)$$

$$u\frac{\partial T}{\partial x} + v\frac{\partial T}{\partial y} = \alpha\left(\frac{\partial^2 T}{\partial y^2}\right) + \frac{Q_0}{\rho C_P}(T - T_\infty)$$
$$+ \tau\left[D_B\left(\frac{\partial T}{\partial y}\frac{\partial C}{\partial y}\right) + \frac{D_T}{T_\infty}\left(\frac{\partial T}{\partial y}\right)^2\right] + \frac{v}{C_P}\left(1 + \frac{1}{\beta}\right)\left(\frac{\partial T}{\partial y}\right)^2 \tag{3}$$

$$u\frac{\partial C}{\partial x} + v\frac{\partial C}{\partial y} = D_B\left(\frac{\partial^2 C}{\partial y^2}\right) + \frac{D_T}{T_\infty}\left(\frac{\partial^2 T}{\partial y^2}\right) \tag{4}$$

where u and v are the velocity over the x and y axis respectively. $\beta = \frac{\mu_B\sqrt{2\pi_C}}{P_y}$ is Casson fluid parameter, σ is the conductivity , α is the thermal diffusivity. D_T and D_B are both the coefficients of several diffusion, Q_0 is the coefficient of the heat sources, C_P is the specific heat, and $\tau = \frac{\rho C_p}{\rho C_f}$ indicates the nanoparticle material'. The boundary

conditions are as follows

$$u = u_w(x) = ax^m, v = v_w, T = T_w(x) = T_\infty + Ax^n, D_B\left(\frac{\partial C}{\partial y}\right)\frac{D_T}{T_\infty}\left(\frac{\partial T}{\partial y}\right)y = 0 \Big\}$$

$$u \to 0, T \to T_\infty, C \to C_\infty, as\ y \to \infty$$

(5)

Now the above equations converted to

$$u = ax^m, g(\eta), v = -ax^{\frac{n-1}{2}}\sqrt{\frac{v}{x}}\left(\left(\frac{n+1}{2}\right)g(\eta) + \frac{n-1}{2}ng'(\eta)\right), \eta = \sqrt{\frac{a}{v}}x^{\frac{n-1}{2}}y \Big\}$$

$$\theta(\eta) = \frac{T - T_\infty}{T_w - T_\infty}, \phi(\eta) = \frac{C - C_\infty}{C_w - C_\infty}$$

(6)

After applying the similarity transformation the governing equations reduced to the following forms.

$$(1 + \frac{1}{\beta})g''' - ng'^2 + \frac{n-1}{2}gg'' - Mg' + G_r\theta(\eta) + G_c\phi(\eta) = 0$$

(7)

$$\frac{1}{pr}\theta'' + \frac{n-1}{2}g\theta' - ng'\theta + \lambda\theta + Nb\theta'\phi' + Nt\theta'^2 + (1 + \frac{1}{\beta})Ecg''^2 = 0$$

(8)

$$\phi'' + \frac{n+1}{2}scg\phi' + \frac{Nb}{Nt}\theta'' = 0$$

(9)

The related conditions are

$$g(0) = g_w, g'(0) = 1, \theta'(0) = -Bi(1 - \theta(0)), Nb\phi'(0) + Nt\theta'(0) = 0, at\ \eta=0 \Big\}$$

$$g'(\infty) \to 0, \theta(\infty) \to 0, \phi(\infty) \to 0\ as\ \eta \to \infty$$

(10)

P_r is the prandtl number, , Ec is Eckert number, Sc is the Schmidt number, f_W is the suction parameter, Biot number is represented as Bi. G_r, G_c is the Grasshoof Numbers Nt and Nb.

Both are used for thermoporesis.

$$pr = \frac{u}{\alpha}, Sc = \frac{v}{D_B}, M = \frac{\sigma B_0^2}{ap}, G_r = \frac{g\beta_T(T_w - T_\infty)}{a^2 x^{n-1}},$$

$$G_c = \frac{g\beta_c(C - C_\infty)}{a^2 x^{n-1}}\ \lambda = \frac{Q_0}{u_w pc_p}$$

$$Nb = \frac{(pc)_p D_B(C_w - C_\infty)}{(pc)_f v}, Ec = \frac{u_w^2}{(T_w - T_\infty)C_p}$$

$$Nt = \frac{(pc)_p D_T(T_w - T_\infty)}{(pc)_f T_\infty v}, f_w = \frac{-2v_w'}{(n+1)a^{\frac{1}{n}}\sqrt{vu_w^{(2n-1)/2n}}}$$

(11)

The measures of functional consideration incorporate the drag power coefficient (C_f), neighborhood Nusselt Nu'_x and

nearby Sherwood numbers, are known as follows:

$$T_w = \mu_B(1 + \frac{1}{\beta})\left(\frac{\partial u}{\partial y}\right)_{y=0}$$

$$q_w = -k\left(\frac{\partial T}{\partial y}\right)_{y=0}$$

$$q_m = -D_B\left(\frac{\partial C}{\partial y}\right)_{y=0}$$

(12)

Substituting Eqs. (7) and (14) into Eq. (13), we obtain

$$Re_x^{1/2} C_{gx} = (1 + \frac{1}{\beta})g'(0)$$

$$Re_x^{-1/2} Nu_x = -\theta'(0)$$

$$Re_x^{-1/2} Sh_x = -\phi'(0)$$

(13)

Wherever $Re_x = \frac{u_w x}{v}$ the local Reynolds number

Numerical analysis of the model

By considering the explicit finite difference method the governing equations are obtained.

$$\left(1+\frac{1}{\beta}\right)\frac{g_{i,j+1}-3g_{i,j}g_{i,j+1}+3g_{i+1,j}g_{i,j}+g_{i+1,j}}{(\Delta x)^3}$$

$$-\eta\frac{g_{i,j+1}-2g_{i,j}+g_{i,j+1}}{(\Delta y)^2}+\frac{\eta+1}{2}\frac{g_{i+1,j}-g_{i,j}}{(\Delta x)}-\frac{g_{i,j+1}-g_{i,j}}{\Delta y}$$

$$-M\frac{g_{i,j+1}-g_{i,j}}{(\Delta x)}+G_r\theta(\eta)+G_c\varphi(\eta)=0 \qquad (14)$$

$$\frac{1}{P_r}\frac{\theta_{i,j+1}-2\theta_{i,j}+\theta_{i,j-1}}{(\Delta x)^2}+\frac{n+1}{2}g\left(\frac{\theta_{i,j}-\theta_{i-1,j}}{\Delta y}\right)$$

$$-ng'\theta+\lambda\theta+N_b\left(\frac{\theta_{i,j}-\theta_{i-1,j}}{\Delta x}\right)\left(\frac{\varphi_{i,j}-\varphi_{i-1,j}}{\Delta y}\right)$$

$$+N_t\frac{\theta_{i,j+1}-2\theta_{i,j}+\theta_{i,j-1}}{(\Delta x)^2}$$

$$+\left(1+\frac{1}{\beta}\right)E_c\frac{g_{i,j+1}-2g_{i,j}+g_{i,j+1}}{(\Delta y)^2}=0 \qquad (15)$$

$$\frac{\varphi_{i,j+1}-2\varphi_{i,j}+\varphi_{i,j-1}}{(\Delta x)^2}+\frac{n+1}{2}S_cg\left(\frac{\varphi_{i,j}-\varphi_{i-1,j}}{\Delta y}\right)$$

$$+\frac{N_b}{N_t}\frac{\theta_{i,j+1}-2\theta_{i,j}+\theta_{i,j-1}}{(\Delta x)^2}=0 \qquad (16)$$

Hence this is the expression of finite difference method of the governing Equations. Where M is the magnetic parameter. E_c Is the Eckert number, P_r is the prandtl number. The boundary Conditions are as follows;

$$U(i,j)=1, V(i,j)=0, \theta'(i,j)=Bi(1-\theta(0)),$$
$$g(i,j)=1, \varphi(i,j)=1 \ at \ y=0,$$

$U(i,j)\to1, \theta(i,j)\to0, g(i,j)\to0, \phi(i,j)\to1$ as $y\to\infty$

Stability and convergence criteria of the model

The Stability and convergence obtained by using finite difference form. α Is the non-Newtonian Casson factor and β is the Casson fluid parameter. The Fourier expansion of U, θ and g separated by $e^{i\alpha x}e^{i\beta y}$ with a constant, Where

$i=\sqrt{-1}$ at $t=g$;

$$U:\psi(\eta)e^{i\alpha x}e^{i\beta y}$$
$$\theta:\theta(\eta)e^{i\alpha x}e^{i\beta y}$$
$$g:g(\eta)e^{i\alpha x}e^{i\beta y}$$

And the changed parameter obtained as follows;

$$U':\psi'(\eta)e^{i\alpha x}e^{i\beta y}$$
$$\theta':\theta'(\eta)e^{i\alpha x}e^{i\beta y}$$
$$g':g'(\eta)e^{i\alpha x}e^{i\beta y}$$

$$\frac{1}{P_r}\frac{2\theta(\eta)(\cos\beta\Delta y-1)}{(\Delta x)^2}+\frac{n+1}{2}g\frac{\theta_{i-1,j}-\theta_{i,j}}{\Delta y}-$$

$$n\frac{2g(\eta)(\cos\beta\Delta y-1)}{(\Delta x)^2}+\lambda\theta+N_b\frac{\theta_{i-1,j}-\theta_{i,j}}{\Delta y}\frac{\varphi_{i-1,j}-\varphi_{i,j}}{\Delta x}$$

$$+N_t\left(\frac{\theta_{i-1,j}-\theta_{i,j}}{\Delta y}\right)^2+\left(1+\frac{1}{\beta}\right)E_c\frac{2g(\eta)(\cos\beta\Delta y-1)}{(\Delta x)^2} \qquad (17)$$

Where $U'=A_1U+A_2\theta+A_3g$

$$A_1=\frac{1}{P_r}\frac{2\theta(\eta)(\cos\beta\Delta y-1)}{(\Delta x)^2},$$

$$A_2=N_t\left(\frac{g(\eta)e^{i\beta\Delta y-1}}{\Delta y}\right),$$

$$A_3=\left(1+\frac{1}{\beta}\right)E_c\frac{2g(\eta)(\cos\beta\Delta y-1)}{(\Delta y)^2}$$

Where A_1, A_2, A_3 is -4,

Hence the stability condition differs the primary condition-

$$U=V=T=C=0$$
$$\Delta\eta=0.007, \Delta x=0.9,$$
$$\Delta y=0.39, E_c\geq0.225,$$
$$P_r\geq0.467, N_t\geq0.556$$

RESULT AND DISCUSSION

To obtain a physical knowledge of the problem, equ (2)-(4) and boundary conditions (5) are converted ODE's to PDE's as equ.(7)-(9) with boundary conditions (10).Further, to obtained the interpretation of the problem, consider the implications of various physical parameter values the magnetic M , thermometric diffusion (Nt), Eckert

number (E_c), heat source ($\sin k$) parameter, Casson β Brownian diffusion Nb, the Prandtl number (P_r), temperature $\theta(\eta)$, the volume fraction, $\phi(\eta)$ drag force($\mathrm{Re}_x^{\frac{1}{2}} C_{fx}$), local Nusselt($\mathrm{Re}_x^{-\frac{1}{2}} Nu_x$) and local Sherwood $\mathrm{Re}_x^{-\frac{1}{2}} Sh_x$ these are numerically and showed through. Introduce the stability and convergence criteria model. Further, governing equations are solved by finite difference method. The fixed values of the various parameters are as follows

$$\beta = 0.5, M = 3.0, \mathrm{Pr} = 0.7, K = 1.0, Ec = 0.5,$$
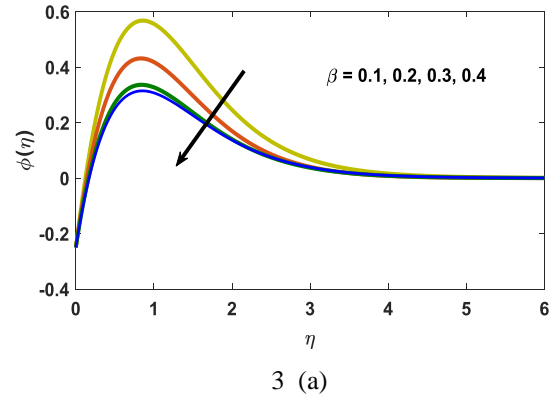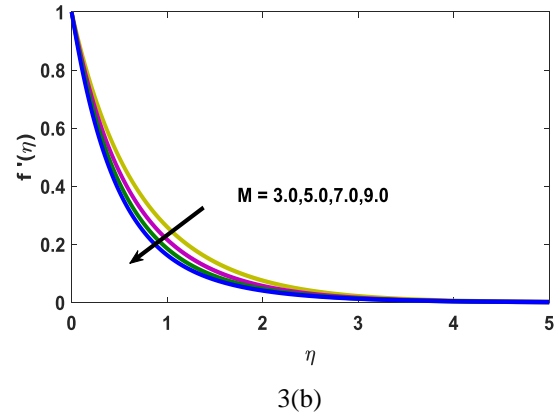$$Nb = 0.6, Nt = 0.5, \lambda = 3, Sc = 0.5$$
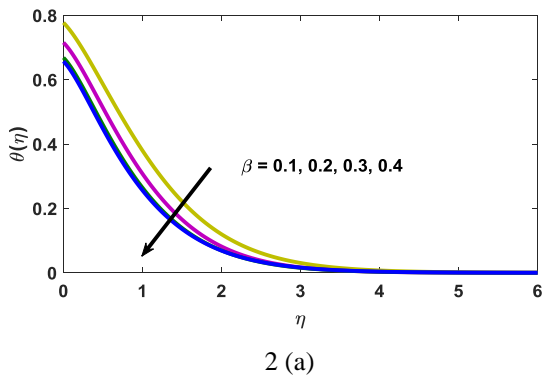
2 (a)
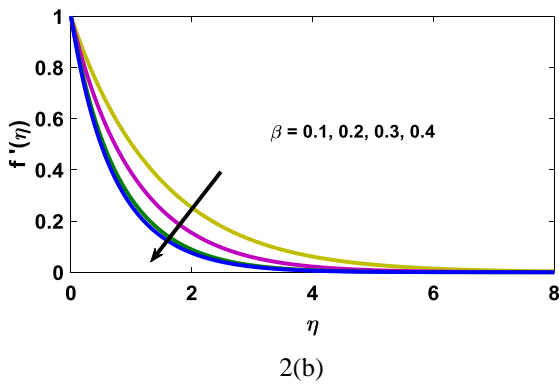
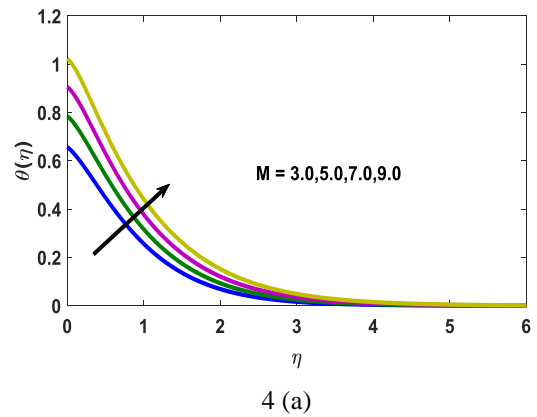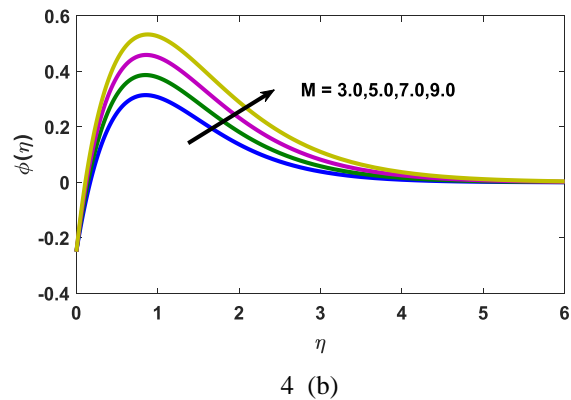
2(b)

Fig.2 (a) Temperature 2(b) Velocity Profiles for β

3 (a)

3(b)

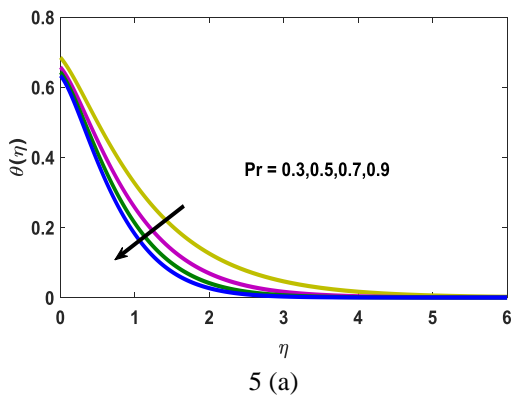**Fig.3 (a) Concentration for β (b) Velocity for M.**

4 (a)

4 (b)

Fig.4 (a) Temperature for M. (b) Concentration for M.

5 (a)
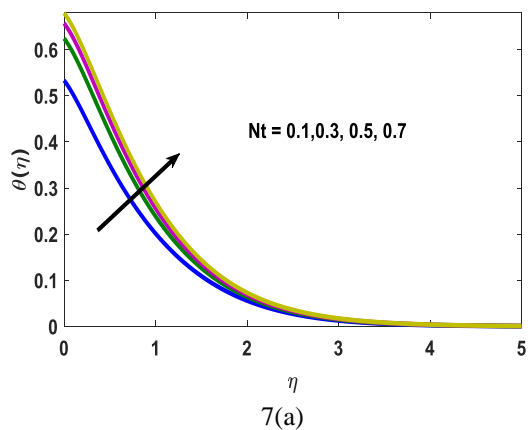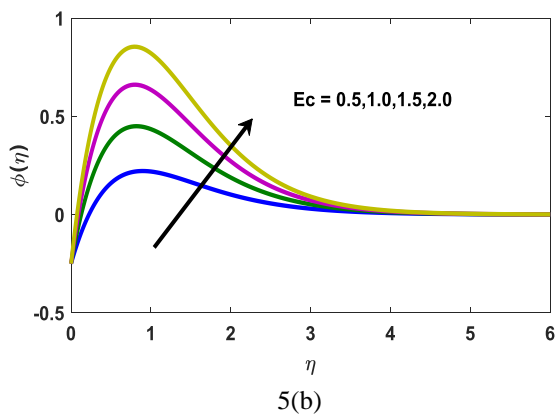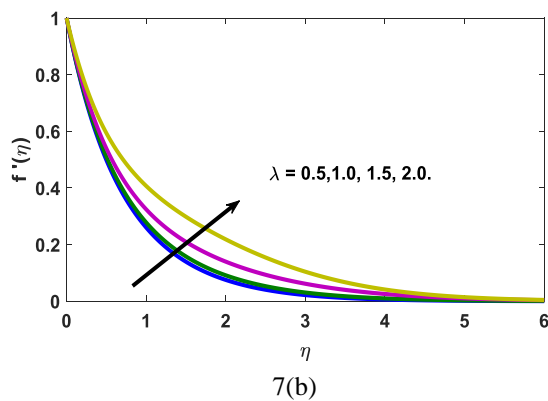
5(b)

Fig.5 (a) Temperature for Pr. **(b) Concentration for** Ec.

7(a)

7(b)

Fig.7 (a) Temperature for Nt **(b) Velocity for** λ

6 (a)
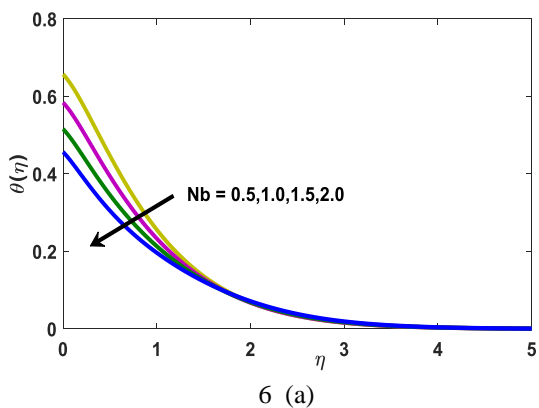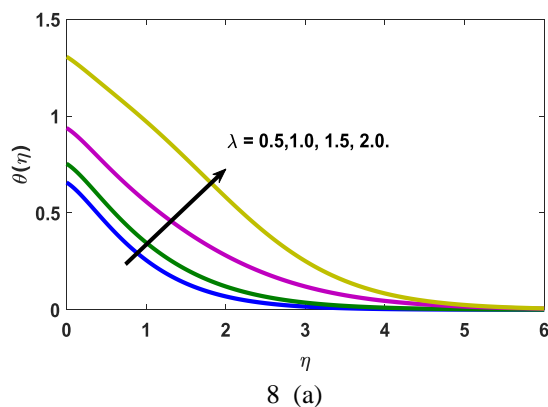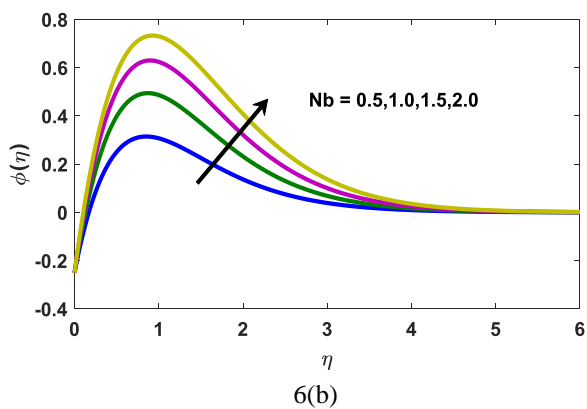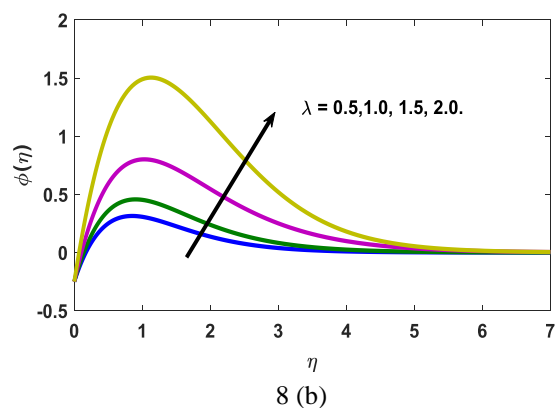
6(b)

Fig.6 (a) Temperature for Nb **(b) Concentration for** Nb.

8 (a)

8 (b)

Fig.8 (a) Temperature for λ **(b) Concentration for** λ

Fig 2(a),Fig.2 (b) and the effect of Casson Parameter(β) on temperature $\theta(\eta)$ is shown to decrease as the casson parameter β increase , so that the decreasing character of the temperature boundary layer thickness as β increases is observed.In Fig 2(b) Cassonfluid parameter β affects velocity and concentration profiles. The effects of Casson parameter β on velocity profiles ($f'(\eta)$) for permeable sheets are shown in Fig. 2b . Velocity is shown to decrease as the Casson parameter β increases. In Fig 3(a), It is apparent that the snowballing of β values improves the concentration distribution. It is also observed that when the β increases, $\phi(\eta)$ decreases.

In Fig 3(b) as the magnetic M parameter increases Physically, the impact of the magnetic value M increases as the Lorentz forces get stronger along the direction perpendicular to the x-axis, providing more resistance in the fluid flows and reducing the velocity profile. It is observed that the flow velocity of nanofluid decreases with the increasing $f'(\eta)$ and M estimations. in Fig 4(a) prepares to detect the effect of the magnetic field on temperature distribution It is demonstrated that as magnetic M increases, the temperature of the fluid rises dramatically. In Fig 4(b) demonstrates the effect of M on $\phi(\eta)$. It is noticed that $\phi(\eta)$ decreases as the value increases, but it increases as the value of M increases. In Fig 5.(a) the effect of P_r on temperature $\theta(\eta)$ is shown to decrease as the P_r increase , so that the decreasing character of the temperature boundary layer thickness as P_r increases is observed. In Fig 5 (b) prepared to observe the effect of the Eckert number (E_c) on temperature distribution $\theta(\eta)$. It is demonstrated that as the Eckert number (E_c) grows, the temperature of the fluid rises dramatically. Physically, the viscosity of a fluid in a viscous flow absorbs kinetic energy from the fluid's motion and converts it into internal energy, which heats the fluid. This operation, known as viscous dissipation, is partially irreversible.

In Fig 6(a) demonstrates the effect of the Brownian Nb parameter on $\theta(\eta)$ It is discovered that is $\theta(\eta)$ decreases with Nb while increases with the parameter.In Fig 6(b), It is worth noting that an increase in Nb enhances the the concentration profile due to suction. In Fig 7(a) consists of the influence of the thermophoresis parameter Nt on the temperature distribution $\theta(\eta)$. The temperature outline with the thickness of the thermal layer is observed to increase with the snowballing values of Nt . Physically, in the thermophoretic effect, nanoparticles move from the heated stretch board to the cool fluid in the environment due to

temperature pattern control. In Fig.7 (b) $\theta(\eta)$ variation with varying amounts of heat source ($\sin k$) λ in a constant worth situation of other parameters is elaborated. It can be seen that the heat source raises the temperature and hence the thickness of the thermal-layer. This is because the heat source ($\sin k$) adds extra heat to the surface, which increases the amount of heat produced in the boundary layer and leads to a higher temperature area.In Fig.8 (a) and Fig.8(b) demonstrates the effect of λ on $\theta(\eta)$ It is observed that $\theta(\eta)$ decreases as the value of increases β , but it increases when the value of λ increases. Skin friction is improving as the growing of β , E_c , Nb , λ value decreases when M , P_r , Nt increased.Heat transfer is enhanced with the constant of M , P_r , E_c , Nb , Nt , λ values are constant when β decreases.Mass transfer is boosted when β is increased while values of M , P_r , E_c , Nb , Nt are decreases.Table.1 is represent the results of skin friction, heat transfer and mass transfer for various parameters.

Table 1 Skin friction,heat and mass transfer				
Parameter	values	Skin friction	Heat transfer	Mass transfer
β	0.1	7.824171	2.750000	25.210248
	0.2	5.942993	1.500000	12.305267
	0.4	4.371352	0.750000	-5.408777
	3.0	4.371352	0.750000	-5.408777
M	5.0	5.015783	0.750000	-6.336210
	7.0	5.581493	0.750000	-7.202313
	9.0	6.091920	0.750000	-8.026566
	0.5	4.357017	0.750000	-4.815631
Pr	0.7	4.371352	0.750000	-5.408777
	0.9	4.374208	0.750000	-5.946244
	1.1	4.372439	0.750000	-6.450418
	0.5	4.445181	0.750000	-4.308661
Ec	1.0	4.267588	0.750000	-6.941015
	1.5	4.111087	0.750000	-9.219842
	2.0	3.972152	0.750000	-11.209436
	0.5	4.371352	0.750000	-5.408777
Nb	1.0	4.332302	0.750000	-6.602221
	1.5	4.304807	0.750000	-7.414328
	2.0	4.284137	0.750000	-7.967239
	0.1	4.186525	0.750000	-10.895543
Nt	0.3	4.340998	0.750000	-6.411361
	0.5	4.371352	0.750000	-5.408777
λ	0.7	4.380191	0.750000	-4.996318
	0.5	4.371352	0.750000	-5.408777
	1.0	4.277513	0.750000	-6.248607

CONCLUSION

The effect of a electrically conducting fluid on an Newtonian casson fluid containing nano particles passing through a wedge through boundary layers was effectively explored. The above equations are converted into ordinary differential equation(ODE) using RK method .Large value of g for flow across the vertical plates and also horizontal plate improve the velocity profile . For the both flows the temperature distribution and nano particle concentration decrease.On the other hand it has been seen that the impact of Brownian motion and thermophoresis on the heat transfer is extremely comparable. Including both Newtonian and Non Newtonian fluid the viscosity of fluid increases due to magnetic field.

❖ Skin friction is improving as the growing of β , E_c , Nb , λ value decreases when M , P_r , Nt increased.

❖ Heat transfer is enhanced with the constant of M , P_r , E_c , Nb , Nt , λ values are constant when β decreases.

❖ Mass transfer is boosted when β is increased while values of M , P_r , E_c , Nb , Nt are decreases.

REFERENCES

[1] Shaw S, Mahanta G, Sibanda P. Non-linear thermal Convection in Casson fluid flow over a horizontal plate with convective boundary conditions. Alexandria Engineering Journal. 2016;55(2):1295-1304.

[2] Das M, Mahanta G, Shaw S, Parida SB. Unsteady MHD Chemically reactive double diffusive Casson fluid past in porous medium with heat and mass transfer. Heat transfer- Asian research 2019;48(5):1761-1777.

[3] Yu H, Qi H, Li K, Zhang J, Xiao P, Wang X. OpenFlow Based Dynamic Flow Scheduling with Multipath for Data Center Networks. Science and Engineering of Computer Systems. 2018; 32(4):251–258.

[4] Zhang K, Liu X, Wan J, Ren Y, Xu BL. Intelligent Automation and Soft Technology. Numerical optimization technique for unsteady rotor flows based on online service. 2019;25(3):527–546.

[5] Mahanta G, Das M, Shaw S, Mahala BK.MHD double-diffusive thermosolutal maragoni convection non-Newtonian Casson fluid flow over a permeable stretching sheet. Heat transfer. 2020;49(4):1788-1807.

[6] Hayat T, Shehzad SA, Alsaedi A, Alhothuali MS. Mixed convection stagnation point flow of Casson fluid with convective boundary conditions. Chinese Physics Letters. 2012;29(11):256-307.

[7] Shehzad SA, Hayat T, Qasim M, Asghar S. Mass transfer effects on Casson fluid MHD flow with suction and chemical reaction. Brazilian Journal of Chemical Engineering. 2013;30(1):187–195.

[8] Mukhopadhyay S, Mondal IC, Chamkha AJ. Casson fluid flow and heat transfer past a symmetric wedge. Heat Transfer—Asian Research. 2013;42(8):665-675.

[9] Pramanik S. In the presence of thermal radiation, casson fluid flow and heat transfer past an exponentially porous stretched surface. Ain Shams Engineering Journal. 2014;(5):205–212.

[10] Mahanta G, Shaw S. Convective boundary conditions with 3D Casson fluid flow via a porous linearly stretched sheet. Alexandria Engineering Journal. 2015;54(3):653–659.

[11] Khalid, Khan I, Khan A, Shafie S. An unsteady MHD free convection flow of Casson fluid passed through a porous material with no oscillating vertical plate. Engineering Science and Technology. 2015;18:309–317.

[12] Mustafa M, Khan JA. Model for Casson nanofluid flow past a non-linearly stretched sheet with magnetic field effects. AIP Advances. 2015;5(7):077148.

[13] Nadeem S, Mehmood R, Akbar NS. Analytical solution for oblique flow of a Casson nanofluid with convective boundary conditions that has been optimized. International Journal of Thermal Sciences. 2014;78:90–100.

[14] Malik MY, Naseer M, Nadeem S, Rehman A. The boundary layer flow of Casson nanofluid over a vertical exponentially stretching cylinder. Applied Nanoscience. 2014;4(7):869-873.

[15] Wahiduzzaman M, Miah MM, Hossain MB, Johora F, Mistri S. MHD Casson fluid flow past a non-isothermal porous linearly stretching sheet. Nonlinear Dyna. And Chaos. 2014;2:61–69.

[16] Sulochana C, Kumar M, Sandeep N. The effects of non-linear thermal radiation and chemical reactions on MHD 3D Casson fluid flow in porous media. Chemical and Process Engineering Research.2015;37:225.

[17] Sarojamma G, Vendabai K. Boundary layer flow of a Casson nanofluid past a vertical exponentially stretching cylinder in the presence of a transverse magnetic field with internal heat generation/absorption. International Journal of Mathematical and Computational Sciences. 2015;9(1):138-43.

[18] Khalid A, Khan I, Khan A, Shafie S. Unsteady MHD free convection flow of Casson fluid past over an oscillating vertical plate embedded in a porous medium. Engineering Science and Technology, an International Journal. 2015;18(3):309-317.

[19] Besthapu P, Bandari S. Mixed convection MHD flow of a Casson nanofluid over a nonlinear permeable stretching sheet with viscous dissipation. Journal of Applied Mathematics and Physics. 2015;3(12):1580.

[20] Imtiaz M, Hayat T, Alsaedi A. Mixed convection flow of Casson nanofluid over a stretching cylinder with convective boundary conditions. Advanced Powder Technology. 2016;27(5):2245-2256.

[21] Oyelakin IS, Mondal S, Sibanda P. Unsteady Casson nanofluid flow over a stretching sheet with thermal radiation, convective and slip boundary conditions. Alexandria Engineering Journal. 2016;55(2):1025–1035.

[22] Afify AA. The influence of slip boundary condition on Casson nanofluid flow over a stretching sheet in the presence of viscous dissipation and chemical reaction. Mathematical Problems in Engineering. 2017.

[23] Ibrahim SM, Lorenzini G, Kumar PV, Raju CS. Influence of chemical reaction and heat source on dissipative MHD mixed convection flow of a Casson nanofluid over a nonlinear permeable stretching sheet. International Journal of Heat and Mass Transfer. 2017;111:346-355.

[24] Shah Z, Kumam P, Deebani W. Radiative MHD Casson Nanofluid Flow with Activation energy and chemical reaction over past nonlinearly stretching surface through Entropy generation. Scientific Reports. 2020;10(1):1-4.

[25] Butt AS, Maqbool K, Imran SM, Ahmad B. Entropy generation effects in MHD Casson nanofluid past a permeable stretching surface. International Journal of Exergy. 2020;31(2):150-171.

[26] Alwawi FA, Alkasasbeh HT, Rashad AM, Idris R. MHD natural convection of Sodium Alginate Casson nanofluid over a solid sphere. Results in physics. 2020;16:102818.

[27] Eid MR, Alsaedi A, Muhammad T, Hayat T. Comprehensive analysis of heat transfer of gold-blood nanofluid (Sisko-model) with thermal radiation. Results in physics. 2017;7:4388-4393.

[28] Shehzad SA, Abdullah Z, Abbasi FM, Hayat T, Alsaedi A. Magnetic field effect in three-dimensional flow of an Oldroyd-B nanofluid over a radiative surface. Journal of Magnetism and Magnetic Materials. 2016;399:97-108.

[29] Eid MR, Mahny KL. Unsteady MHD heat and mass transfer of a non-Newtonian nanofluid flow of a two-phase model over a permeable stretching wall with heat generation/absorption. Advanced Powder Technology. 2017;28(11):3063-73.

[30] Eid MR, Alsaedi A, Muhammad T, Hayat T. Comprehensive analysis of heat transfer of gold-blood nanofluid (Sisko-model) with thermal radiation. Results in physics. 2017;7:4388-93.

[31] Eid MR. Time-dependent flow of water-NPs over a stretching sheet in a saturated porous medium in the stagnation-point region in the presence of chemical reaction. Journal of Nanofluids. 2017;6(3):1185–1193.

[32] Hady FM, Ibrahim FS, Abdel-Gaied SM, Eid MR. Radiation effect on viscous flow of a nanofluid and heat transfer over a nonlinearly stretching sheet. Nanoscale Research Letters. 2012;7(1):229.

[33] Eid MR. Chemical reaction effect on MHD boundary-layer flow of two-phase nanofluid model ove

[34] r an exponentially stretching sheet with a heat generation. Journal of Molecular Liquids. 2016;220:718-725.

[35] Muhammad T, Lu DC, Mahanthesh B, Eid MR, Ramzan M, Dar A. Significance of Darcy-Forchheimer porous medium in nanofluid through carbon nanotubes. Communications in Theoretical Physics. 2018;70(3):361.

[36] Al-Hossainy AF, Eid MR, Zoromba MS. SQLM for external yield stress effect on 3D MHD nanofluid flow in a porous medium. Physica Scripta. 2019;94(10):105208.

[37] Eid MR, Al-Hossainy AF, Zoromba MS. FEM for blood-based SWCNTs flow through a circular cylinder in a porous medium with electromagnetic radiation. Communications in Theoretical Physics. 2019;71(12):1425.

[38] Shamshuddin MD, Eid MR. Magnetized nanofluid flow of ferromagnetic nanoparticles from parallel stretchable rotating disk with variable viscosity and thermal conductivity. Chinese Journal of Physics. 2021;74:20-37.

[39] Eid MR, Mahny KL, Dar A, Muhammad T. Numerical study for Carreau nanofluid flow over a convectively heated nonlinear stretching surface with chemically reactive species. Physica A: Statistical Mechanics and its Applications. 2020;540:123063.

[40] Khan N, Riaz I, Hashmi MS, Musmar SA, Khan SU, Abdelmalek Z, Tlili I. Aspects of chemical entropy generation in flow of Casson nanofluid between radiative stretching disks. Entropy. 2020;22(5):495.

[41] Eid MR. Effects of NP shapes on non-Newtonian bio-nanofluid flow in suction/blowing process with convective condition: Sisko model. Journal of Non-Equilibrium Thermodynamics. 2020 Apr 1;45(2):97-108.

[42] Mahanta, G. Shaw, S.Nayak,M.K. Pati,J.C., Effects on MHD Casson stagnation point flow with stability analysis over the stretchering surface with velocity slip. IJAER 2021;16(9):823-829.